Smooth Sliding Mode Control Based Technique of an Autonomous Underwater Vehicle Based Localization Using Obstacle Avoidance Strategy

Fethi Demim[1][a], Abdenebi Rouigueb[2][b], Hadjira Belaidi[3][c], Ali Zakaria Messaoui[4], Khadir Lakhdar Bensseghieur[4], Ahmed Allam[5], Mohamed Akram Benatia[2], Abdelmadjid Nouri[6] and Abdelkrim Nemra[1]

[1]*Laboratory of Guidance and Navigation, Ecole Militaire Polytechnique, Bordj El Bahri, Algiers, Algeria*

[2]*Laboratory of Artificial Intelligence and Virtual Reality, Ecole Militaire Polytechnique, Bordj El Bahri, Algiers, Algeria*

[3]*Signals and Systems Laboratory, Institute of Electrical and Electronic Engineering, University M'Hamed Bougara of Boumerdes, Algeria*

[4]*Laboratory of Complex Systems Control and Simulators, Ecole Militaire Polytechnique, Bordj El Bahri, Algiers, Algeria*

[5]*Ecole Nationale Polytechnique, Algiers, Algeria*

[6]*Department of Maritime Engineering, Université des Sciences et de la Technologie, USTO, Oran, Algeria*

Keywords: Localization, Sonar Data Fusion, Autonomous Underwater Vehicle, Sliding Mode Control.

Abstract: Navigating underwater environments presents serious challenges in control and localization technology. The successful navigation of uncharted territories requires autonomous maneuvers that achieve goals while avoiding obstacles, posing a significant problem to be addressed. Detection-based control using sensor data and obstacle avoidance technology are vital for the autonomy of Autonomous Underwater Vehicles (AUVs). This study focuses on developing a control method based on Sliding Mode Control (SMC) and utilizing an imaging sonar sensor for obstacle avoidance. The proposed approach includes a controller for pitch and depth control, enabling avoidance of stationary objects. A Gaussian potential function is employed to guide the AUV's maneuvers and avoid obstructions. Numerous simulation results evaluate the control performance of the AUV in realistic simulation conditions, assessing accuracy and stability. The experimental in simulation results demonstrate the excellent performance of our approach in navigating various obstacles such as gentle rise, steep drop-off, and underwater walls, using seafloor environment simulation models.

1 INTRODUCTION

A comprehensive understanding of the marine environment is crucial for optimal performance in submarine warfare, anti-mine precautions, and offshore area control. Autonomous Underwater Vehicles (AUVs) have evolved into advanced platforms capable of executing various tasks without human intervention, such as ocean exploration and minefield detection (Breivik and Fossen, 2000). AUVs can operate independently, making them valuable for marine research and warfare applications citeBlidberg03. The history of underwater vehicles dates back to the 18th century, with submarines and torpedoes as the first autonomous underwater vehicles (Issac et al., 1979) (Desa et al., 2001). The increasing prevalence of AUVs is driven by their capabilities and potential for future advancements in ocean exploration and research.

Small AUVs are compact, self-contained vehicles designed with minimal drag, featuring a single underwater DC power thruster. They depend on onboard computers, power sources, and payload equipment for self-governing control, navigation, and guidance. These AUVs can be outfitted with sophisticated sensors to analyze oceanic characteristics or specialized payloads for tracking moving ma-

[a] https://orcid.org/0000-0003-0687-0800
[b] https://orcid.org/0000-0001-5699-2721
[c] https://orcid.org/0000-0003-2424-626X

Demim, F., Rouigueb, A., Belaidi, H., Messaoui, A., Bensseghieur, K., Allam, A., Benatia, M., Nouri, A. and Nemra, A.
Smooth Sliding Mode Control Based Technique of an Autonomous Underwater Vehicle Based Localization Using Obstacle Avoidance Strategy.
DOI: 10.5220/0012118200003543
In *Proceedings of the 20th International Conference on Informatics in Control, Automation and Robotics (ICINCO 2023) - Volume 1*, pages 529-537
ISBN: 978-989-758-670-5; ISSN: 2184-2809
Copyright © 2023 by SCITEPRESS – Science and Technology Publications, Lda. Under CC license (CC BY-NC-ND 4.0)

rine organisms. While AUVs have previously operated semi-autonomously under human oversight, significant strides towards full autonomy have been achieved, as documented in (Issac et al., 1979).

Currently, AUVs have found extensive use in mapping and surveying tasks since their inception in the 1970s. Notably, the HUGIN series, developed by Kongsberg Maritime and the Norwegian Defense Research Establishment, stands out as a highly successful commercial AUV platform. Nevertheless, AUVs face challenges related to navigation, communication, autonomy, and endurance, with a strong focus on enhancing autonomy in ongoing research. Various control techniques are applied for distinct operations, encompassing pitch and depth control, tracking and formation control, and obstacle avoidance strategies that make use of forward-looking sonar for detecting and evading static obstacles (Desa et al., 2001), (Coleman, 2003), (Issac et al., 1979).

In both land and sea environments, the hurdle of obstacle avoidance presents significant difficulties for robots. Ground robots can execute maneuvers like stop-back-turn, but underwater vehicles face unique complications due to the necessity of halting forward momentum and maintaining a stationary position (Healey and Kim, 2000). This challenge has implications for the autonomy and navigation of Autonomous Underwater Vehicles (AUVs) ((Desa et al., 2001). Particularly in uncharted territories, AUVs grapple with the complexities of adhering to programmed waypoints, thus driving the exploration of artificial intelligence techniques to dynamically navigate around obstacles in the dynamic marine environment (Coleman, 2003). Moreover, the current designs of AUVs reveal limitations in their ability to adapt to various littoral conditions (Blidberg, 2003).

The Indian Underwater Robotics Society (IURS), founded by Indian students abroad, introduced autonomous underwater vehicle technology to India with the creation of BhAUV in 2005 (Li and Xiao, 2005). Subsequently, IURS advanced their efforts by developing a cost-effective AUV named Jal, which is equipped with navigational sensors, sonar, and computer vision capabilities. Similarly, the National Institute of Oceanography (NIO) in Goa made strides in 2009 by launching Maya, a compact autonomous underwater vehicle designed for oceanic data collection (Prestero, 2009). Moreover, the Central Mechanical Engineering Research Institute (CMERI) played a pivotal role in India's autonomous underwater vehicle development, producing a versatile platform capable of tasks such as mapping, surveillance, mine countermeasures, and oceanographic measurements, even in challenging weather conditions (Li and Xiao, 2005) and (Prestero, 2009).

Navigating underwater vehicles while avoiding obstacles presents multifaceted challenges related to autonomy, nonlinear modeling, and environmental uncertainties. Researchers have explored diverse control strategies, including Sliding Mode Control (SMC), Fuzzy Logic Control (FLC), and Backstepping, to tackle these complexities. Advancements like pseudo-spectral methods, Rapidly-exploring Random Trees (RRT), and Probabilistic RoadMap (PRM) have elevated trajectory planning and control precision, enhancing overall performance. Nevertheless, existing trajectory planning methods often overlook dynamic constraints, curtailing optimization and tracking capabilities. To surmount this, a refined mathematical model is recommended to attain more accurate and trackable navigation trajectories. These innovations have the potential to substantially elevate AUV performance, especially in dynamic underwater conditions.

In this study, the central focus centers on devising a control methodology that leverages SMC alongside imaging sonar sensors for precise pitch and depth control, specifically geared towards obstacle avoidance. The integration of these advanced techniques aims to enhance AUV maneuverability and navigation accuracy, contributing to safer and more effective underwater operations.

The article is structured into distinct sections. Section II covers AUV modeling, encompassing kinematic and dynamic equations. In Section III, the utilization of SMC for obstacle avoidance is elucidated, employing sonar technology to identify obstacles in the AUV's trajectory. It details the AUV's depth adjustment to navigate a new path based on obstruction height and range data. Section IV showcases experimental outcomes validating the effectiveness of the proposed approach. Finally, Section V offers concluding remarks, suggesting potential avenues for future work.

2 AUV SYSTEM MODEL

2.1 Kinematic and Dynamic Modeling

The AUV used in this work is treated as a rigid body, assuming minimal deflections during movement. The acceleration of the earth has negligible impact on the car's center of mass, as noted by (Healey and Kim, 2000). The primary forces acting on the AUV include inertial, gravitational, hydrostatic, propulsion, thruster, and hydrodynamic forces from lift and drag, as explained by (Healey and Kim, 2000). Euler rota-

tion angles (ϕ, θ, ψ) are used to specify the AUV's orientation relative to the global reference frame. These rotations are commonly known as yaw, pitch, and roll for submersibles. The transformation matrix $f(.)$ facilitates translation between the global and local reference frames.

$$f(.) = \begin{bmatrix} c\theta c\psi & c\psi s\theta s\phi - s\psi c\phi & c\psi s\theta c\phi + s\psi s\phi \\ c\theta s\psi & s\psi s\theta s\phi + c\psi c\phi & s\psi s\theta c\phi - c\psi s\phi \\ -s\theta & s\phi c\theta & c\phi c\theta \end{bmatrix} \quad (1)$$

where c and s represent $\cos(.)$ and $\sin(.)$ successively.

Translational motion of AUVs occurs in 3D space, where it can move along three linear axes: surge (u_x), sway (v_y), and heave (w_z), corresponding to the x, y, and z directions, respectively (see Figure 1(a)). The relationship between global position $[X; Y; Z]$ and local linear velocities $[u_x; v_y; w_z]$ can be expressed by a transformation equation.

$$\begin{bmatrix} u_x \\ v_y \\ w_z \end{bmatrix} = f(\phi, \theta, \psi) \times \begin{bmatrix} \dot{X} \\ \dot{Y} \\ \dot{Z} \end{bmatrix} \quad (2)$$

The AUV model includes angular velocities that are transformed and summed to determine the total angular velocity $[\dot{\phi}; \dot{\theta}; \dot{\psi}]$, expressed as local components $[p_x; q_y; r_z]$. The Motion Reference Unit (MRU) sensor provides roll, pitch, and yaw rates in the body frame, as well as body accelerations. With high update rates, the MRU sensor determines the AUV's position $[X, Y; Z]$, velocity $[u_x; v_y; w_z]$, and attitude $[\phi; \theta; \psi]$, among other data (Demim et al., 2018), (Demim and et al., 2019), and (Demim et al., 2022a).

$$\begin{bmatrix} \dot{\phi} \\ \dot{\theta} \\ \dot{\psi} \end{bmatrix} = \begin{bmatrix} 1 & \sin(\phi)\tan(\theta) & \cos(\phi)\tan(\theta) \\ 0 & \cos(\phi) & -\sin(\phi) \\ 0 & \sin(\phi)\cos(\theta) & \cos(\phi)\cos(\theta) \end{bmatrix} \begin{bmatrix} p_x \\ q_y \\ r_z \end{bmatrix} \quad (3)$$

Dynamics and control of mobile robotic vehicles provides a total of six equations of motion, each of which is derived from either the rotation or translation of the vehicle.

$$\begin{aligned} X_f &= m[\dot{u}_x - v_y r_z + w_z q_y - x_G(q_y{}^2 + r_z{}^2) + y_G \\ &\quad (p_x q_y - \dot{r}_z) + z_G(p_x r_z + \dot{q}_y)] + (W - B)\sin(\theta) \end{aligned} \quad (4)$$

$$\begin{aligned} Y_f &= m[\dot{v}_y - u_x r_z - w_z p_x + x_G(p_x q_y + \dot{r}_z) - y_G(p_x{}^2 \\ &\quad + r_z{}^2) + z_G(q_y r_z + \dot{p}_x)] - (W - B)\cos(\theta)\sin(\phi) \end{aligned} \quad (5)$$

$$\begin{aligned} Z_f &= m[\dot{w}_z - u_x q_y + v_y p_x + x_G(p_x r_z - \dot{q}_y) + y_G(qr \\ &\quad + \dot{p}_x) - z_G(p_x{}^2 + q_y{}^2)] + (W - B)\cos(\theta)\cos(\phi) \end{aligned} \quad (6)$$

$$\begin{aligned} K_f &= I_x \dot{p}_x + (I_z - I_y) q_y + I_{xy}(p_x r_z - \dot{q}_y) - I_{yz}(q_y{}^2 \\ &\quad - r_z{}^2) - I_{xz}(p_x q_y + \dot{r}_z) + m[y_G(\dot{w}_z - u_x q_y + v_y p_x) \\ &\quad - z_G(\dot{v}_y + u_x r_z - w_z p_x)] - (y_G W - y_B B)\cos(\theta) \\ &\quad \cos(\phi) + (z_G W - z_B B)\cos(\theta)\sin(\phi) \end{aligned} \quad (7)$$

$$\begin{aligned} M_f &= I_y \dot{q}_y + (I_y - I_z) p_x - I_{xy}(q_y r_z + \dot{p}_x) + I_{yz}(p_x q_y \\ &\quad - \dot{r}_z) + I_{xz}(p_x{}^2 - r_z{}^2) - m[x_G(\dot{w}_z - u_x q_y + v_y p_x) \\ &\quad - z_G(\dot{u}_x - v_y r_z + w_z q_y)] - (x_G W - x_B B) \\ &\quad \cos(\theta)\cos(\phi) + (z_G W - z_B B)\sin(\theta) \end{aligned} \quad (8)$$

$$\begin{aligned} N_f &= I_z \dot{r}_z + (I_y - I_x) p_x - I_{xy}(p_x{}^2 - q_y{}^2) - I_{yz}(p_x r_z \\ &\quad - \dot{q}_y) + I_{xz}(q_y r_z - \dot{p}_x) + m[x_G(\dot{v}_y + u_x r_z - w_z p_x) \\ &\quad - y_G(\dot{u}_x - v_y r_z + w_z q_y)] - (x_G W - x_B B) \\ &\quad \cos(\theta)\sin(\phi) - (y_G W - y_B B)\sin(\theta) \end{aligned} \quad (9)$$

where

- W represents the weight; B for Buoyancy; I for mass moment of inertia terms; u_x, v_y, w_z are the component velocities, and p_x, q_y, r_z represent the component angular velocities for body fixed systems.
- x_B, y_B, z_B represent the position difference between geometric center and center of buoyancy; x_G, y_G, z_G are the position difference between geometric center and center of gravity, and X_f, Y_f, Z_f, K_F, M_f, N_f represent the sums of all external forces operating in a given body's fixed direction.

This study focuses on the vertical plane motion of the diving system, examining the observed state variables $(x(t) = w_z, q_y, \theta, Z)$. The presented equations model the diving system's response to control surface deflections, with constant forward velocity. The accuracy of the model's predictions may vary due to factors like water conditions, system dynamics, and control surface performance. However, it may not fully capture the system's response to changes in forward velocity or other external factors. The simplified diving equations of motion for pitch and depth control are as follows:

$$\dot{x}(t) = M^{-1}Ax(t) + M^{-1}(B\delta_s(t) + E) \quad (10)$$

$$\begin{bmatrix} \dot{w}_z(t) \\ \dot{q}_y(t) \\ \dot{\theta}(t) \\ \dot{z}(t) \end{bmatrix} = M^{-1}A \begin{bmatrix} w_z(t) \\ q_y(t) \\ \theta(t) \\ Z(t) \end{bmatrix} + M^{-1}(B\delta_s(t) + E) \quad (11)$$

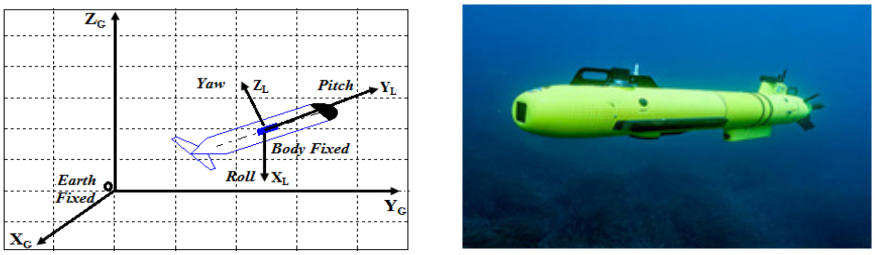

(a) (b)

Figure 1: Experimental model of the AUV: (a) AUV model presentation, (b) Photo of AUV model.

where:

$$M = \begin{bmatrix} (m - Z_{\dot{w}_z}) & -Z_{\dot{q}_y} & 0 & 0 \\ -M\dot{w}_z & (I_{yy} - M_{\dot{q}_y}) & 0 & 0 \\ 0 & 0 & 1 & 0 \\ 0 & 0 & 0 & 1 \end{bmatrix} \quad (12)$$

$$A = \begin{bmatrix} Z_{w_z} & (mU_0 + Z_q) & 0 & 0 \\ Mw_z & M_q & (z_B B - z_G W) & 0 \\ 0 & 1 & 0 & 0 \\ 1 & 0 & U_0 & 0 \end{bmatrix} \quad (13)$$

$$B = \begin{bmatrix} Z_\delta \\ M_\delta \\ 0 \\ 0 \end{bmatrix}, \quad E = \begin{bmatrix} (W - B) \\ 0 \\ 0 \\ U_{cz} \end{bmatrix} \quad (14)$$

The state matrix $x(t)$ includes observed variables: vertical velocity $w_z(t)$, pitch rate $q_y(t)$, pitch angle $\theta(t)$, and depth $Z(t)$. The mass matrix M includes the vehicle's mass and derivatives of hydrodynamic forces and moments with respect to state variables. Matrices A and B consist of hydrodynamic coefficients linking state variables to control surface deflection. Matrix E accounts for the vehicle's weight and buoyancy difference, and stern plane deflection control is denoted as $\delta_s(t)$. The model may not accurately reflect the diving system's response to changes in forward velocity or other external factors due to a constant forward velocity.

2.2 Sonar Observation Model

The AUV's vertical sonar sensor rotates a fan-shaped beam incrementally to scan a 2D plane (Demim et al., 2022a). Detected obstacles are represented by $[\rho;\ \theta]$ parameters. The AUV monitors its altitude and collects sonar data up to 90 meters for seafloor contours. A sliding mode controller maintains depth. Using a Gaussian potential function, the AUV modifies its trajectory based on processed sonar images to avoid collision with previewed obstacles. To ensure sufficient front sonar range, the staves of the sonar housing are tilted back at $\beta = 60°$ (Figure 2), and the front sonar operates at low frequency. In this case, the observation model for AUVs operating in structured environments and using sonar to detect obstacles can be defined as follows (Demim et al., 2022a):

$$\begin{bmatrix} \rho_i \\ \theta_i \end{bmatrix} = \begin{bmatrix} \sqrt{(x - x_m)^2 + (z - z_m)^2} \\ \sin^{-1}\left[\frac{z - z_m}{\rho_j}\right] \end{bmatrix} + \varepsilon_{\rho_j, \theta_j} \quad (15)$$

where

- In the simulation, x and z represent the AUV's position with respect to the X and Z axes in the global frame, while x_m and z_m refer to the x-coordinate and altitude of the AUV in the global frame, respectively;
- $[\rho_i;\ \theta_i]$ represent the range and bearing, respectively, to the i^{th} obstacle in the environment relative to the AUV pose. Additionally, ρ_j denotes the measured range in the local frame;
- $\varepsilon_{\rho_j, \theta_j}$ defines a zero-mean white noise.

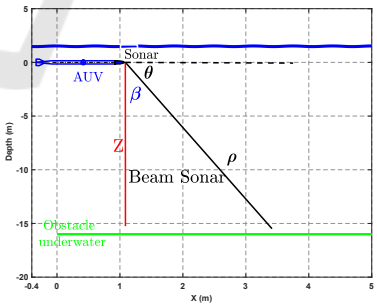

Figure 2: Diagram of the sonar used by AUV.

The simulation represented the seafloor using limited equally spaced points in the XZ plane. The simulated front sonar records range and bearing for each point, which vary over time depending on the AUV's location in the XZ plane. The AUV's dynamic controller directs the avoidance trajectory to ensure safe navigation over the ascending seafloor, considering obstacle range and height based on the AUV's current position.

3 OBSTACLE AVOIDANCE TECHNIQUE

Potential fields are essential for robot obstacle avoidance in dynamic environments, guiding the robot's movement with varying potential primitives. Using a local representation of the environment based on previous data reduces noise, especially with sonar data (Khatib, 1986). This approach is also practical for AUVs, where the goal generates attractive potential, and obstacles create repulsive potentials, allowing the AUV to navigate safely. Gradients represent forces attracting the AUV towards the goal, akin to negatively charged particles (Khatib, 1986) (Belker and Schulz, 2002). Combining attractive forces towards the goal with repulsive forces from obstacles, the AUV can safely navigate to its destination in a 2D plane with position $Q = (x,\ y)$ in R^2 space.

The AUV's movement is controlled by an artificial potential field, a scalar function $U(q):\ R^2 \rightarrow R$, with q representing the robot's position in 2D space. The function combines attractive and repulsive potentials (U_{att} and U_{rep}) respectively. The AUV's current position is denoted by $Q = (x,\ y)$, while its target location is $Q_{goal} = (x_g;\ y_g)$. The attractive force begins affecting the AUV even before it reaches the goal, increasing as the distance to the target decreases. Once the AUV reaches its destination, the attractive force disappears.

$$U(Q) = U_{att}(Q) + U_{rep}(Q) \tag{16}$$

The repulsion potential is the result of the superposition of the repulsive potentials generated by the obstacles which is represented by:

$$U(Q) = U_{att}(Q) + \sum_i U_{rep_i}(Q) \tag{17}$$

The potential field $U(Q)$ combines attractive potential U_{att} and repulsive potential U_{rep} from obstacles, represented by U_{rep_i}. The gradient of the potential field, $\nabla U(Q)$, points in the direction of maximum increase in $U(Q)$. The AUV navigation method employs attractive and repulsive potentials to guide the AUV's movement. The negative gradient of the artificial potential acts as the propelling force for the AUV (Belker and Schulz, 2002).

$$F(Q) = -\nabla U_{att}(Q) - \nabla U_{rep}(Q) \tag{18}$$

The vector force $F(Q)$ in Eq. 18 decreases locally towards the maximum U and points in the direction of the AUV. It acts as the velocity vector that propels the AUV. The attractive field can be described as a parabolic function.

$$U_{att}(Q) = \frac{1}{2}\xi P^2_{goal}(Q) \tag{19}$$

With ξ a positive scalar and P_{goal} the Euclidean distance $\|Q - Q_{goal}\|$. The function $U_{att}(Q)$ is therefore positive or zero and reaches its minimum at Q_{goal} where $U_{att}(Q_{goal}) = 0$.
The F_{att} force is represented as follows (Belker and Schulz, 2002):

$$\begin{aligned} F_{att}(Q) &= -\nabla U_{att}(Q) = -\xi P_{goal}(Q)\nabla P_{goal}(Q) \\ &= -\xi(Q - Q_{goal}) \end{aligned} \tag{20}$$

Figure 3(a) illustrates the repulsive potential for two obstacles, while Figures 3(b) and 3(c) show the attractive and repulsive potentials, respectively. Figure 3(d) depicts the sum of these potentials. The repulsive force acts along the line connecting the AUV and obstacle, directed towards the AUV. The resulting force $F(Q)$ can be expressed as:

$$F(Q) = F_{att}(Q) + F_{rep}(Q) \tag{21}$$

In a dynamic two-dimensional space (depicted in Figure 4), a force model is formulated, involving distinct repulsive forces (F_{rep1} and F_{rep2}) from obstacles collectively pushing away the AUV. Additionally, an attractive force (F_{att}) from a target point contributes to the resulting force F through superposition. The environment in Figure 3 is intentionally designed to minimize local optima. Our approach combines FLC with LOS guidance, enhancing trajectory planning robustness. Unlike the potential method susceptible to local minima, our FLC-based strategy avoids suboptimal outcomes by adaptively adjusting control parameters. While sonar for shape capture faces challenges in representing obstacle rears, our method employs reverse sonar motion and diverse data angles to gradually overcome this limitation and achieve comprehensive representation.

4 CONTROL BASED METHOD

4.1 Sliding Mode Controller Design

Underwater robotic vehicles face stability challenges in dynamic environments, involving waves, wind, and currents. Autopilots and onboard sensors help stabilize motion, but incomplete sensor data can create state uncertainty, necessitating observation theory for state reconstruction. This experiment's AUV was equipped with a Sliding Mode Controller (SMC) for its robustness in handling nonlinear behavior (Healey, 2001). SMC simplifies modeling of underwater nonlinear systems, defining a sliding surface that combines state variables (position, velocity, and acceleration) and reduces them to satisfy $S = 0$ (Demim

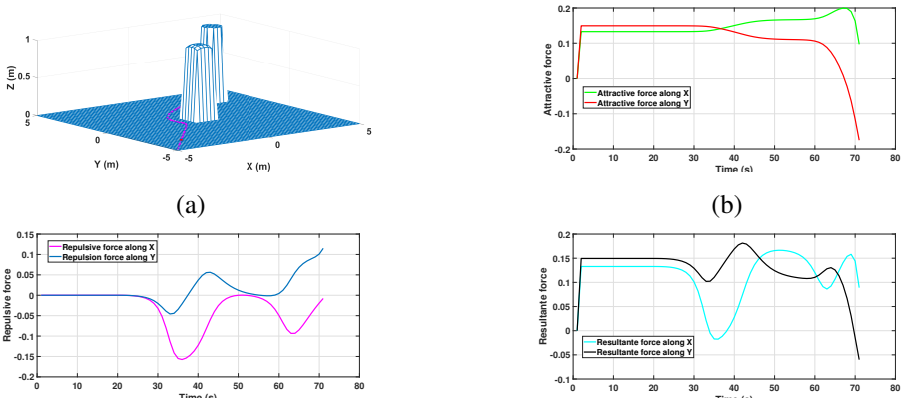

Figure 3: Potential field presentation: (a) Repulsive potential for two obstacles, (b) Attractive potential, (c) Repulsive potential, (d) Resultant potential.

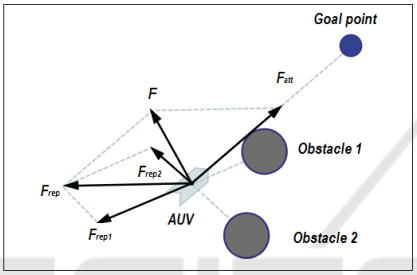

Figure 4: AUV's resulting force model.

et al., 2022b). This approach is crucial for AUVs in confined underwater environments, requiring stability, maneuverability, and quick obstacle avoidance responses.

$$S = \dot{\tilde{x}} + \lambda\tilde{x} \tag{22}$$

where $\tilde{x} = x - x_d$ is the tracking error and $\lambda > 0$ is the control bandwidth. When $S = 0$, this equation represents a sliding surface that exhibits exponential dynamics:

$$\tilde{x}(t) = \exp(-\lambda(t - t_0))\tilde{x}(t_0) \tag{23}$$

The goal is to find a nonlinear control law ensuring the tracking error $\tilde{x}(t)$ converges to zero within finite time, with the sliding mode $S = 0$. Regardless of the initial condition $\tilde{x}(t_0)$, the error trajectory will reach the time-varying sliding surface in finite time and then slide exponentially towards $\tilde{x}(t) = 0$. Achieving this control objective involves designing an appropriate nonlinear control law.

$$\lim_{t\to\infty} S(t) = 0 \tag{24}$$

Defining a virtual reference x_u is useful in the development of the sliding control law:

$$\dot{x}_u = \dot{x}_d - \lambda\tilde{x} \Rightarrow S = \dot{x} - \dot{x}_u \tag{25}$$

Therefore, the expression for $m\dot{S}$ can be derived as follows:

$$\begin{aligned} m\dot{S} &= m\ddot{x} - m\ddot{x}_u = (u - d|\dot{x}|\dot{x}) - m\ddot{x}_u \quad (26)\\ &= -d|\dot{x}|S + (u - m\ddot{x}_u - d|\dot{x}|\dot{x}_u) \quad (27)\end{aligned}$$

Let's examine a possible function candidate that resembles a scalar Lyapunov function:

$$V(S,t) = \frac{1}{2}mS^2, \quad m > 0 \tag{28}$$

SMC defines a sliding surface S as a scalar function that linearly combines state variables (position, velocity, and acceleration). The goal is to continuously reduce the state variables until they satisfy $S = 0$. For a second-order nonlinear system, the sliding surface can be defined as shown in the equation provided, where λ is an unknown frequency in radians per second. SMC aims to achieve robustness and stability in controlling nonlinear systems. To define the control law u, a positive definite function $V(S) > 0$ with a negative derivative for all times greater than zero is established using Lyapunov methods, as described in the works of Healey (Healey and Kim, 2000) (Healey, 2001). Conditions on the switching gain K are fond by requiring that $\dot{V} \leq 0$.

$$u = \{b(\dot{\tilde{x}}) + K\tilde{x}\} - \lambda\dot{\tilde{x}} - \eta sat(S/\phi) \tag{29}$$

where K is a parameter that affects the behavior of the control law, $b(\dot{\tilde{x}})$ represents the damping force applied to the system, which is proportional to the velocity of the state error, $K\tilde{x}$ represents the feedback force applied to the system, which is proportional to the state error, and $\lambda\dot{\tilde{x}}$ and $\eta sat(S/\phi)$ represent additional damping and saturation forces, respectively, that further adjust the control input. A saturation function is introduced to mitigate chattering in estimated states

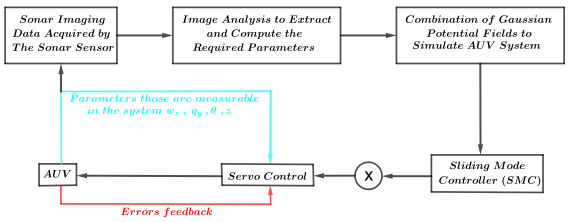

Figure 5: Schematic of AUV's sliding mode controller.

during high-frequency switching scenarios. An AUV experiment, featuring a simulated MRU and imaging sonar, collected data to monitor the AUV's depth within a few meters. Employing a Gaussian potential function and an SMC controller with parameters from processed sonar data, the AUV adjusted its trajectory to avoid collisions by adapting its path based on obstacle locations in sonar images (Figure 5). The SMC controller offers advantages in underwater settings, handling nonlinear behaviors and simplifying system modeling, but challenges such as noise, sensor malfunctions, and external disturbances need attention. The AUV experiment demonstrated stability, maintaining cruising height and avoiding collisions using sonar images. Additional research is required to assess SMC performance underwater, accounting for noise and sensor failures.

5 SIMULATION RESULTS AND DISCUSSION

5.1 Computational Domains for Pitch Case Using CFD Interface

Using computational domains is essential in AUV pitch analysis with CFD. A second domain simulates different angles for diving and rising (Fig. 6). This rectangular, parallelepiped-shaped domain extends by 1L before the bow and 2 L after the stern, with width 1 L and height 1.33 L, providing enough space for maneuvering. CFD helps analyze fluid flow around the AUV, crucial in underwater vehicle design and control.

5.2 Experimental Validation of SMC Control for AUV

This study presents an AUV obstacle avoidance technique involving pitch and depth control. Front sonar detects obstacles such as coral reefs or sea barriers to prevent path obstruction. The AUV adjusts pitch angle and depth for obstacle navigation. The sliding mode controller computes an alternate path, pitching up to the barrier's height while maintaining distance. Upon clearing the obstacle's top, the AUV returns to its original course by pitching down on the downward slope. The sonar triggers the algorithm and supplies obstruction size and range information. MATLAB simulations utilized a developed sonar model to generate 2D images. Three seafloor types were explored to address diverse mission scenarios.

The method simulates AUV navigation with sonar-guided control, adjusting pitch and depth using a 2D domain. Different seafloor profiles are compared. Sonar and MRU collaboratively enable the AUV to autonomously navigate, avoiding obstacles and maintaining course.Figure compares proposed marine environment simulations with different seafloor profiles. The AUV employs sonar beams, generating images (Figures 9, 11, and 13) for obstacle detection. The MRU and sonar jointly provide a comprehensive view of the AUV's surroundings, enabling autonomous navigation, obstacle avoidance, and course maintenance.

The method initially employs potential field-based pitch and depth control for obstacle avoidance. However, Figure 8 reveals oscillatory response issues, necessitating AUV repositioning. Introducing sliding mode control enhances efficiency and stability in obstacle avoidance. SMC adjusts pitch and depth upon obstacle detection, enabling safe navigation and improved overall motion control for the AUV. By employing SMC, the AUV achieves precise and stable trajectory, unaffected by external factors like ocean currents or waves. As shown in Figure 9, the AUV maintains a safe 90 m distance from a 4 m high obstacle, effectively clearing it. Upon reaching the obstacle's top, pitch adjustment returns the AUV to its original altitude. This method presents a promising solution for AUV obstacle avoidance, enhancing navigation in intricate and changing underwater environments.

The AUV effectively avoids collision, ascending the barrier at approximately 33 m from the global origin, despite a slight delay in the obstacle avoidance SMC controller's depth adjustments. Crucial obstacle location and distance information is obtained from front sonar images (Figure 10), assisting the AUV's trajectory adaptation. While response delay is noted, successful collision avoidance demonstrates a promising step towards improved and reliable AUV obstacle avoidance methods.

Figure 11 accurately portrays obstacle height and distance. The AUV's controller adjusts stern surfaces, pitching the vehicle upward upon encountering the obstacle. The Gaussian potential field guides

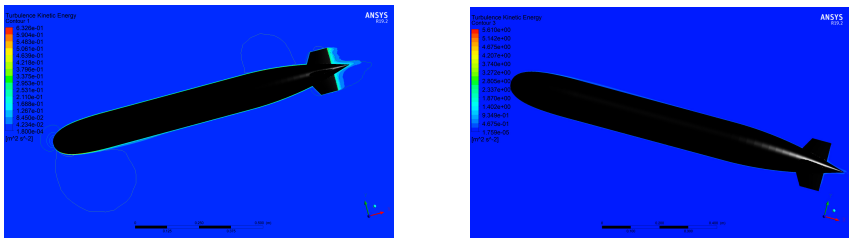

(a) (b)

Figure 6: Computational domain for pitch case: (a) Diving case, (b) Rising case.

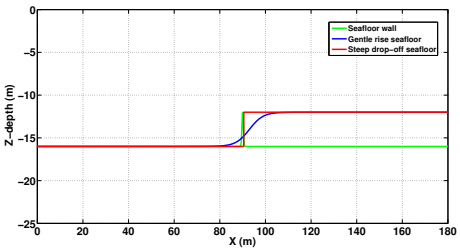

Figure 7: Comparison of marine environment models.

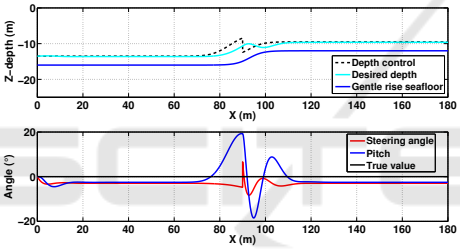

Figure 8: Analysis of AUV navigation dynamics along gentle seafloor rise.

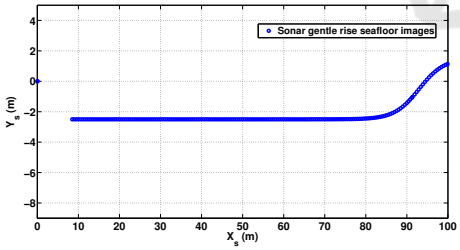

Figure 9: Observe sonar images of gentle seafloor rise.

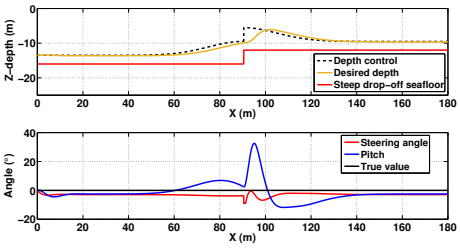

Figure 10: Analyzing the dynamics of AUV navigation on steep seafloor drop-off.

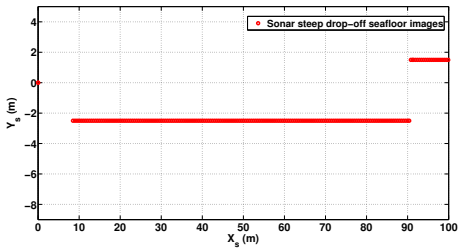

Figure 11: Observe seafloor sonar images with steep drop-off.

the AUV to a level altitude and its original trajectory. This field's attractive and repulsive forces effectively steer the AUV to avoid obstacles, altering its path. Real-time data from sonar sensors is essential for precise obstacle navigation in the environment.

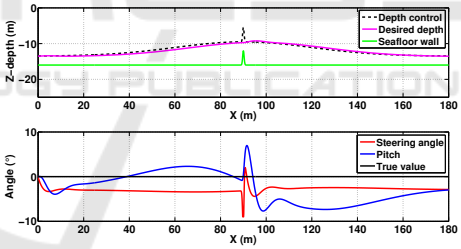

Figure 12: Analysis of AUV navigation dynamics along seafloor wall.

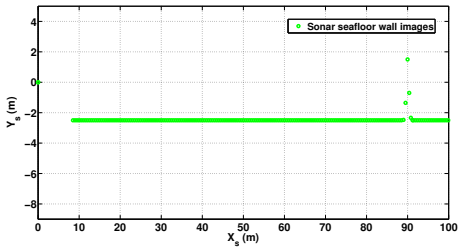

Figure 13: Observe sonar images of the seafloor wall.

The combination of the Gaussian potential field and sonar sensors effectively enables AUV obstacle avoidance in both simulations and real-world scenarios. This strategy ensures reliable navigation in intricate underwater environments, as evidenced in Figure

12. The SMC controller employs an internal Gaussian potential field, facilitating the AUV's maneuverability around significant obstacles. By adjusting stern control surfaces, the controller induces controlled pitching within $\pm 8^{\circ}$ range. The AUV follows the potential field's guidance until it successfully clears the obstacle.

Figure 13 illustrates a trajectory that, though impractical due to the AUV's limited maneuverability and response time, emphasizes the potential field method's effectiveness in obstacle avoidance. The method rapidly generates energy-based fields for real-time obstacle avoidance, complemented by processed front sonar images. Nonetheless, limitations exist, such as addressing local minima, concave obstacles, and AUV oscillations in confined spaces. Simulations validate its proficiency in navigating structured environments like seafloor walls.

6 CONCLUSIONS

This article delves into the obstacle avoidance abilities of autonomous underwater vehicles through front sonar sensors in the vertical plane. The research proposes a sliding mode controller coupled with imaging sonar to establish Gaussian potential fields, demonstrating efficient obstacle avoidance. While the study showcases successful outcomes, validation through real sonar data across varied marine environments is essential. The article suggests the utilization of multiple sonar sensors for a comprehensive 3D field of view, aiming to eliminate blind spots.

Future AUV control research should prioritize improving model accuracy and reliability. Enhancements can involve extending the model to cover additional motion planes and fine-tuning existing control systems. Integrating data from multiple sensors can mitigate real-time state estimation uncertainties. Waypoint navigation remains vital for autonomous AUV control, with sliding mode controllers offering stabilizing capabilities for roll, pitch, altitude, and velocity tracking while managing estimated errors.

REFERENCES

Belker, T. and Schulz, D. (2002). Local action planning for mobile robot collision avoidance. In *Intelligent Robots and System, IEEE/RSJ International Conference*, pages 601–606.

Blidberg, D. (2003). The development of autonomous underwater vehicles (auv). In *A Brief Summary, Autonomous Undersea Systems Institute, Lee New Hampshire, USA*.

Breivik, M. and Fossen, T. (2000). Guidance laws for autonomous underwater vehicles. In *Norwegian University of Science and Technology, Norway*.

Coleman, J. (2003). Undersea drones pull duty in iraq hunting mines. In *Cape Code Times*.

Demim, F., Benmansour, S., Nemra, A., Rouigueb, A., Hamerlain, M., and Bazoula, A. (2022a). Simultaneous localization and mapping for autonomous underwater vehicle using a combined smooth variable structure filter and extended kalman filter.

Demim, F. and et al., A. N. (2019). *NH-∞-SLAM algorithm for autonomous underwater vehicle*.

Demim, F., Nemra, A., Abdelkadri, H., Louadj, K., Hamerlain, M., and Bazoula, A. (2018). Slam problem for autonomous underwater vehicle using svsf filter. In *Proceeding of 25th IEEE International Conference on Systems, Signals and Image Processing, Maribor, Slovenia*, pages 1–5.

Demim, F., Rouigueb, A., Nemra, A., Bouguessa, R., and Chahmi, A. (2022b). A new filtering strategy for target tracking application using the second form of smooth variable structure filter. In *Proceedings of the Institution of Mechanical Engineers, Part I: Journal of Systems and Control Engineering*.

Desa, E., Madhan, R., and Maurya, P. (2001). Potential of autonomous underwater vehicles as new generation ocean data platforms. In *National Institute of Oceanography, Dona Paula, India*.

Healey, A. (2001). Dynamics and control of mobile robotic vehicles. In *Class Notes, Naval Postgraduate School, Monterey, California, Winter*.

Healey, A. and Kim, J. (2000). Control and random searching with multiple robots. Proceedings IEEE CDC Conference, Sydney Australia.

Issac, M., Adams, S., He, M., Neil, W., Christopher, D., and Bachmayer, R. (1979). Manoeuvring experiments using the mun explorer auv. In *In proceeding*.

Khatib, O. (1986). Real-time obstacle avoidance for manipulators and mobile robots.

Li, X. and Xiao, J. (2005). Robot formation control in leader-follower motion using direct lyapunov method.

Prestero, T. (2009). Verification of a six-degree of freedom simulation model of remus autonomous underwater vehicle. In *MIT and WHOI*.